DOI: 10.1002/ejic.201001125

Novel Metal-Organic Frameworks Incorporating [$Cp°_2Mo_2P_4S$] ($Cp° = 1\text{-}t\text{Bu-3,4-}Me_2C_5H_2$), P_4S_3 and Cu_2I_2 Building Blocks

Christian Gröger,[a] Hans Robert Kalbitzer,[a] Michael Pronold,[b] Dmitry Piryazev,[c,d] Manfred Scheer,[b] Joachim Wachter,*[b] Alexander Virovets,[c] and Manfred Zabel[b]

Keywords: Metal-organic frameworks / Coordination polymers / Molybdenum / Copper / Phosphorus / Sulfur

The synthesis and characterization of [$Cp°_2Mo_2P_4S$] (**1**) and [$Cp°_2Mo_2P_2S_3$] (**2**) ($Cp° = 1\text{-}t\text{Bu-3,4-}Me_2C_5H_2$) has been described. The reaction of **1** in CH_2Cl_2 with 2 equiv. of CuI in MeCN under diffusion conditions gave [$(Cp°_2Mo_2P_4S)_3(CuI)_4]_n$ (**6a**). The crystal structure of **6a** consists of helical substructures of opposed chirality which are formed by the coordination of two Cu_2I_2 rings to three phosphorus atoms of the *cyclo*-P_4S middle deck of **1**. The resulting helix is connected with four helices of the same chirality by front-backside P coordination of another **1** unit. Compound **6a** can reversibly include or release CH_2Cl_2 molecules without loosing its crystalline character. Thus, storing crystals of **6a** under CH_2Cl_2 results in the formation of **6a**·$0.55CH_2Cl_2$ (**6b**), the unit cell volume increasing by 113.6 $Å^3$ per formula unit, while in high vacuum the unit cell volume of **6b** decreases to the value of **6a**. The reaction of **1** with CuI in the presence of P_4S_3 gave a mixture of two isomeric polymers **7** and **8** of composition [$(Cp°_2Mo_2P_4S)(P_4S_3)(CuI)_2]_n$. The crystal structures of both compounds **7** and **8** contain linear strands of [**1**$(CuI)_2]_n$ and [$(P_4S_3)(CuI)_2]_n$ with planar Cu_2I_2 rings as common interface. A two-dimensional framework is formed by interpenetration of both types of strands. The analogous reaction of the mixture of [$Cp^{\star}_2Mo_2P_4S$] ($Cp^{\star} = C_5Me_5$) and P_4S_3 with CuI gave [$(Cp^{\star}_2Mo_2P_4S)(P_4S_3)(CuI)_2]_n$ (**9**). Contrary to the structures of **7** and **8** in this compound coordination of adjacent P atoms of the η^3-P_3 ligand and the η^2-PS dumbbell leads to the formation of one-dimensional ribbons.

Introduction

There is much actual interest in the assembly of coordination polymers from copper halides and organic Lewis bases.[1] In particular linkers with N,[2] P,[3] S or Se[4] atoms play an important role for the construction of supramolecular organic-inorganic hybrid materials with interesting physical properties. Recent developments focus on the simultaneous coordination of bifunctional P,N[5] or S,N[6] containing organic ligands. Surprisingly little is known about the coordination properties of bifunctional P,S ligands. A prominent example of a multifunctional inorganic P,S ligand is the P_4S_3 cage molecule. While it is possible to involve one to four P atoms in copper coordination,[7] the realization of simultaneous coordination of sulfur and phosphorus by a metal ion has been achieved only with Ag[WCA] compounds (WCA = weakly coordinating anion).[8]

Bis(cyclopentadienylmolybdenum) tripledecker complexes containing a *cyclo*-$P_{5-n}S_n$ (n = 1, 3) middle deck (Scheme 1)[9] are potential organometallic building blocks for the construction of supramolecular networks with copper(I) halides. This has been shown for the first time by the P,S ligand complex [$Cp^*_2Mo_2(\mu,\eta^{3:3}\text{-}P_3)(\mu,\eta^{2:2}\text{-PS})$] ($Cp^*$ = η^5-C_5Me_5),[9] which forms a one-dimensional polymer with CuI.[10] In this compound P atoms in the positions 1 and 4 (Scheme 2) are involved in coordination, whereas the participation of sulfur has been excluded by spectroscopic means. A further example of P,S tripledecker complexes is [$Cp^*_2Mo_2(\mu,\eta^{2:2}\text{-PS})_2S$], in which the coexistence of two η^2-PS ligands and a singly bridging sulfur ligand has been established in the form of two positional isomers **A** and **B** (Scheme 1).[11] No efforts have been made so far to combine two such different types of multifunctional ligands like [$Cp^*_2Mo_2P_4S$] and P_4S_3 by copper halide building blocks. It was also our intention to influence the formation of potential polymers by replacing the Cp^* ligand by Cp° ($Cp° = 1\text{-}t\text{Bu-3,4-}Me_2C_5H_2$). Apart from the synthesis and characterization of [$Cp°_2Mo_2P_2S_3\cdot\{W(CO)_5\}_2$] the Cp° ligand has been employed thus far only in group 5 metallocene chemistry.[12] As a result of this study we describe the formation of an unprecedented helical framework from [$Cp°_2Mo_2P_4S$] (**1**) and copper(I) iodide and the formation of novel inorganic-organometallic hybrid polymers from a mixture of **1** or [$Cp^*_2Mo_2P_4S$] with P_4S_3 as competing connector ligands and CuI.

---

[a] Institut für Biophysik und Physikalische Biochemie der Universität Regensburg,
93040 Regensburg, Germany
[b] Institut für Anorganische Chemie der Universität Regensburg,
93040 Regensburg, Germany
Fax: +49-941-943-4439
E-mail: Joachim.Wachter@chemie.uni-regensburg.de
[c] Nikolaev Institute of Inorganic Chemistry SB RAS,
Ak. Lavrentiev prosp. 3, Novosibirsk 630090, Russia
[d] Novosibirsk State University,
Pirogova str. 2, Novosibirsk 630090, Russia

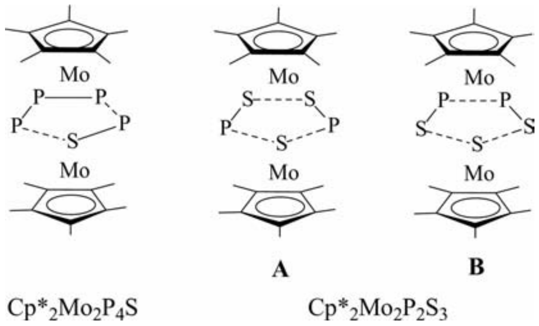

Scheme 1. Examples of tripledecker complexes with *cyclo*-$P_{5-n}S_n$ (n = 1, 3) middle deck.[9,12]

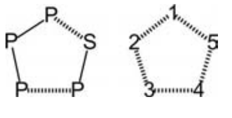

Scheme 2. Connectivities and positions of main group atoms within the middle deck of [$Cp^*_2Mo_2P_4S$].[9,10]

Results and Discussion

Synthesis of [$Cp^\circ_2Mo_2P_{5-n}S_n$] (n = 1, 3)

The reaction of [$Cp^\circ Mo(CO)_2]_2$ with P_4S_3 in boiling toluene gave dark red [$Cp^\circ_2Mo_2P_4S$] (**1**), bright red [$Cp^\circ_2Mo_2P_2S_3$] (**2**), yellow [$Cp^\circ Mo(CO)_2P_3$] (**3**), red [$Cp^\circ_2Mo_2(CO)_4P_2$] (**4**), and dark brown [$Cp^\circ_3Mo_3(CO)_2P_3S_4$] (**5**) [Equation (1)]. All compounds are sensitive towards air and moisture. The composition of complexes **1**–**5** has been confirmed by mass spectrometry and elemental analyses. The ^{31}P NMR spectrum of **1** in C_6D_6 is similar to that of the related compound [$Cp^*_2Mo_2P_4S$], for which the presence of a $\mu,\eta^{3:3}$-P_3- and a $\mu,\eta^{2:2}$-PS ligand has been established.[9]

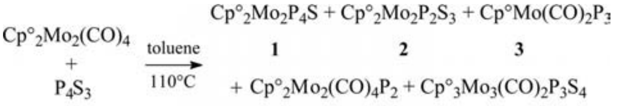

$$\begin{array}{c} \mathrm{Cp^\circ_2Mo_2(CO)_4} \\ + \\ \mathrm{P_4S_3} \end{array} \xrightarrow[110\,^\circ\mathrm{C}]{\text{toluene}} \begin{array}{l} \underset{\mathbf{1}}{\mathrm{Cp^\circ_2Mo_2P_4S}} + \underset{\mathbf{2}}{\mathrm{Cp^\circ_2Mo_2P_2S_3}} + \underset{\mathbf{3}}{\mathrm{Cp^\circ Mo(CO)_2P_3}} \\ + \underset{\mathbf{4}}{\mathrm{Cp^\circ_2Mo_2(CO)_4P_2}} + \underset{\mathbf{5}}{\mathrm{Cp^\circ_3Mo_3(CO)_2P_3S_4}} \end{array} \qquad (1)$$

The ^{31}P NMR spectrum of **2** in C_6D_6 (20 °C) reveals a singlet at δ = –58.4 ppm, which remains invariable down to –110 °C (CD_2Cl_2/[D_8]THF). This means a shift of 20 ppm to high field compared to [$Cp^*_2Mo_2P_2S_3$]. The ^{31}P MAS NMR spectrum of **2** exhibits a group of signals centered at δ = –62.1 ppm (Figure 1). This indicates the existence of different conformations of both cyclopentadienyl rings with respect to the P_2S_3 middle deck in the solid state (Scheme 3), whereas in solution there is a rapid rotation of the Cp° rings. By contrast, the ^{31}P MAS NMR spectrum of [$Cp^\circ_2Mo_2P_2S_3\cdot\{W(CO)_5\}_2$] exhibits only one sharp signal at δ = –63.8 ppm.[11] The crystal structure determination of the latter revealed an eclipsed conformation of Cp° ligands and the $W(CO)_5$ fragments coordinated at P atoms in positions corresponding to isomer **A** (Scheme 3). Thus, in this diadduct the correlation of spectroscopic with crystallographic data is in agreement with the existence of only one conformer even in the solid state.[11]

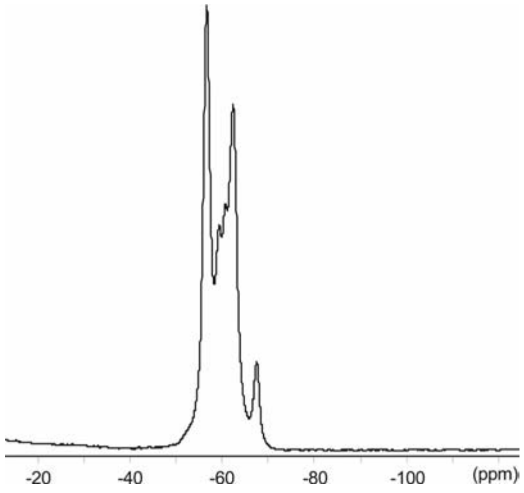

Figure 1. ^{31}P MAS NMR spectrum (121.49 MHz) of **2**. Spinning frequency 30 kHz, MAS probe 2.5 mm.

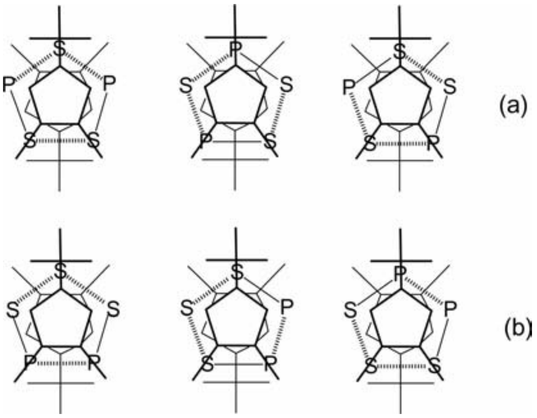

Scheme 3. Staggered conformations of the Cp° ligands with respect to the *cyclo*-P_2S_3 middle deck of **2**. Positional isomers **A** (a) and **B** (b) are considered.

Spectroscopic data of **3** and **4** are analogous to those of related compounds with C_5H_5 and Cp* ligands.[9,13,14] The trinuclear complex **5** is an interesting by-product, which crystallizes from benzene. Its composition follows from mass spectrometry and X-ray diffraction analysis and is supported by spectroscopic data. The IR spectrum shows two strong ν_{CO} frequencies at 1918 and 1830 cm^{-1}. The ^1H NMR spectrum reveals three singlets for the *t*Bu groups, three signals for the methyl groups and five multiplets (2:1:1:1:1) for the ring hydrogens. This pattern is in agreement with three inequivalent Cp° rings. The ^{31}P NMR spectrum in C_6D_6 reveals a doublet at δ = –120.8 ppm and a triplet at δ = 253.3 ppm in a ratio of 2:1 ($^2J_{P-P}$ = 19 Hz).

Striking feature of the $Cp^\circ_2Mo_2$ tripledecker structure is the middle-deck, which consists of two $\mu,\eta^{2:2}$-PS dumbbells (averaged P–S bond lengths 2.055 Å) and a dimetalla-dithiophosphinato ligand (Figure 2). The sulfur atoms of this ligand act as a chelating 3-electron ligand for a Cp°Mo(CO)$_2$ fragment, thus extending the complex chemistry of organodithiophosphinates.[15] The tripledecker unit of **5** may formally be derived from **2A** if one replaces the singly bridging sulfur atom by P3 including the attached fragment (Scheme 1).

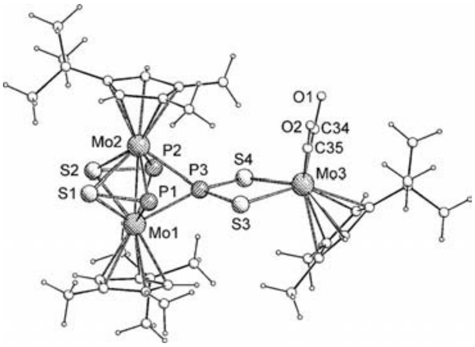

Figure 2. Molecular structure of **5**. Selected distances [Å]: Mo1–Mo2 2.625(1), Mo1–P1 2.464(1), Mo1–P2 2.467(1), Mo1–P3 2.438(1), Mo1–S1 2.490(1), Mo1–S2 2.5635(1), Mo3–S3 2.518(1), Mo3–S4 2.519(1), P1–S1 2.060(2), P2–S2 2.049(2), P3–S3 2.080(2), P3–S4 2.081(3), P1···P3 2.634(2), P2···P3 2.604(2), S1···S2 2.936(2).

Copper(I) Iodide Coordination Polymers

[(Cp°$_2$Mo$_2$P$_4$S)$_3$(CuI)$_4$]$_n$

The reaction of **1** with CuI in the molar ratio 1:2 gave [(Cp°$_2$Mo$_2$P$_4$S)$_3$(CuI)$_4$]$_n$ (**6a**). Dark brown prisms, which are insoluble in common solvents, were obtained by the diffusion method. The composition was determined by X-ray diffraction analysis and has been confirmed by elemental analysis. The ^{31}P MAS NMR spectrum reveals broad and superposed resonances because of the presence of eight non-equivalent phosphorus atoms (see below).

Compound **6a** crystallizes in the space group $I4_1/a$. The crystal structure may be described by a three-dimensional network, which contains at first glance folded four-membered Cu$_2$I$_2$ rings and tripledecker molecules. There are two crystallographically different organometallic linkers which exhibit two different coordination modes with respect to the Cu$_2$I$_2$ rings. "Tripledecker 1" coordinates through P1, P2, and P3 corresponding to the positions 1, 2, and 4 in the middle deck. The structure refinement revealed, that S1 of the PS dumbbell P1–S1 is pointing in two directions (S1 and S1a) and thus forcing the third P atom of the P$_3$ unit also in two positions (P4 and P4a). These two orientations were refined to be present in a ratio of 62:38. "Tripledecker 2" coordinates through positions 1 (P6) and 4 (P5) (Figure 3) to Cu$_2$I$_2$. Because the $\bar{4}$ axis of the space group runs diagonally through the P$_4$S-ring of this tripledecker unit and none of these atoms lie exactly on this axis, all atoms appear twice in a 50:50 ratio. Due to the fact, that the middle deck is attached to Cu$_2$I$_2$ rings, only minor dislocations between the two orientations are allowed and observed.

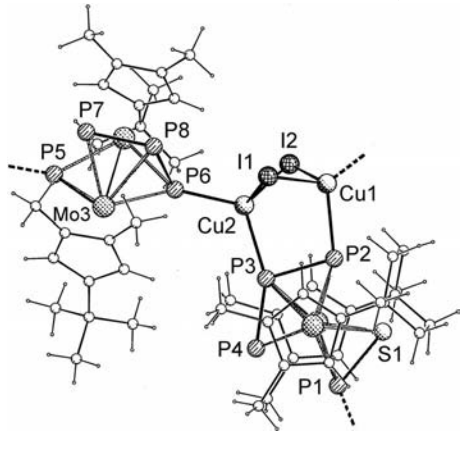

Figure 3. Section of the crystal structure of **6a**; S2 is covered by Mo3. P1, P4 and S1 represent 62%, P7, P8, and S2 50% of the disordered main group atoms. Selected distances [Å] and angles [°]: Mo–Mo$_{\text{mean}}$ 2.677(1), Mo–S 2.481(3)–2.532(6), Mo–P 2.384(6)–2.590(8), S1–P1 2.183(7), S1···P2 2.722(1), S2–P5 2.053(7), P1···P4 2.802(1), P2–P3 2.217(4), P3–P4 2.165(6), P6–P8 2.148(6), P7–P8 2.163(6), Cu1–P1 2.250(2), Cu1–P2 2.339(2), Cu2–P3 2.372(3), Cu2–P6 2.223(5), Cu2–P5 2.243(5), Cu–I$_{\text{mean}}$ 2.672(2), Cu1···Cu2 2.691(2); Cu1–P2–P3 100.9(1), Cu2–P3–P2 90.6(1).

The *cyclo*-P$_4$S middle deck of "tripledecker 1" coordinates through vicinal atoms P2 and P3 of the P$_3$ ligand to both Cu atoms of the folded Cu$_2$I$_2$ ring. The corresponding Cu1–Cu2 distance is shortened to 2.691 Å. Additionally, P1 of the PS dumbbell coordinates to Cu1 of the Cu$_2$I$_2$ ring of the next asymmetric unit. The assignment of P1 in the dumbbell follows from correlation of spectroscopic and X-ray crystallographic investigations in 1D-[(Cp*$_2$Mo$_2$P$_4$S)$_2$(CuI)$_3$]$_n$,[10] which excludes the participation of sulfur as coordination site. If one continues the alternating assembly of "tripledecker 1" and Cu$_2$I$_2$ rings a one-dimensional helix is formed, which completes its repeat unit of 19.9 Å by repetition of four asymmetric units (Figure 4 (top)) around the 4_1 axis of the space group.

The "tripledecker 2" coordinates through P5 of the PS dumbbell and P6 of the P$_3$ ligand. The resulting front-backside coordination allows the connection of two opposed Cu$_2$I$_2$ four-membered rings, which are part of two separate helices of the same sense (Figure 4 (middle)). Accordingly, a central helix is connected with four helices of the same chirality. Following the space group symmetry, the "tripledecker 2" at $z + 1/2$ is acting in the same way, but now the connected helices possess opposite chirality with respect to the first group, running around the 4_3 axis. The resulting crystal structure may then be described by a primitive packing of helical strands, in which adjacent strands have opposite handiness (Figure 4 (bottom)).

Helical structures for (CuX)$_n$ chains are already known,[16] as well as the helical arrangement of an S,N ligand around a linear (CuI)$_n$ chain.[6c] The helical structure of **6a** is unique in a sense that the fundamental building blocks are forced by steric constraints. The structure contains holes with some residual electron density, which seems to be large enough for inclusion of solvent molecules, nei-

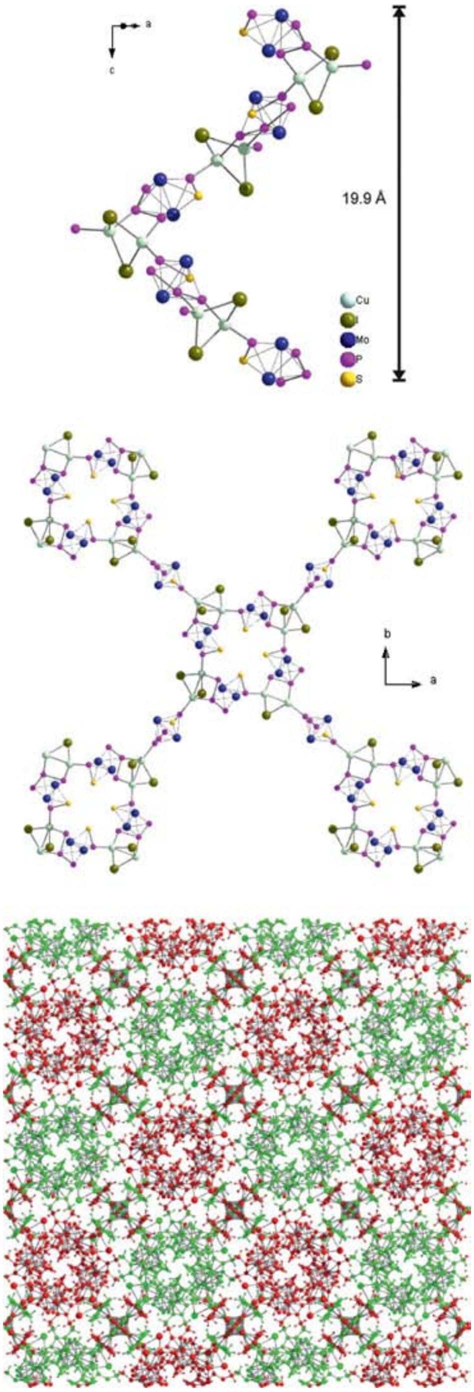

Figure 4. Top: section of the left-handed helix of **6a**. Shown is a repeat unit, Cp° rings are omitted for clarity. Middle: assembly of left-handed helices of **6a** in the lattice. Cp° rings are omitted for clarity. Bottom: view of the 3D-network of **6a** along the *c*-axis. Left-handed helices are red, right-handed helices are green.

ther with residual electron density maps nor by the program SQUEEZE[17] reasonable electron maxima or electron numbers could be found. Compound **6a** can reversibly include CH_2Cl_2 molecules without loosing its crystalline character. After storing crystals of **6a** under CH_2Cl_2 they incorporate solvent molecules in the inter-chain voids resulting in the formation of **6a**·0.55CH_2Cl_2 (**6b**). This inclusion is accompanied by a unit cell volume increasing by 113.6 Å^3 per formula unit. It is noteworthy that the single crystals keep their quality during the process. In high vacuum (8 h) the unit cell volume of **6b** decreases to the value of **6a**. The crystals keep their shape and their diffraction pattern still shows quite nice single separated reflections that can be easily indexed in the smaller unit cell. Therefore, the couple **6a/6b** represents an interesting example of porous metal-organic polymeric compound that can reversibly absorb CH_2Cl_2 without losing its crystallinity.

The influence of the Cp° ligand on the formation of the helical network in **6** is evident by a comparison with the well investigated reaction of [$Cp^*_2Mo_2P_4S$] with CuX (X = Cl, Br, I): The products of composition [$(Cp^*_2Mo_2P_4S)_2(CuX)_3]_n$ are one-dimensional polymers in which linear strands of alternating organometallic [$Cp^*_2Mo_2P_4S$] building blocks and $(CuX)_3$ clusters bear pending [$Cp^*_2Mo_2P_4S$] units, which are coordinated by the *exo*-P atom of the P_3 ligand (Figure 5).[10] One may speculate that the unusual side-on coordination of the Cu_2I_2 ring to adjacent P atoms of the P_3 ligand in **6a/6b** may lead to the helical folding of an originally linear structural motif.

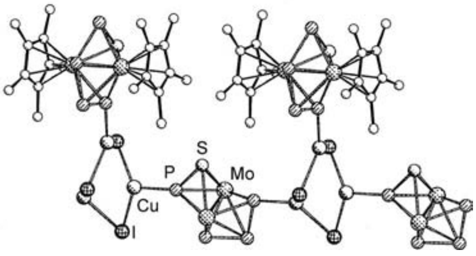

Figure 5. Section of 1D-[$(Cp^*_2Mo_2P_4S)_2(CuI)_3]_n$.[10] H atoms are omitted for clarity in the pending units of [$Cp^*_2Mo_2P_4S$] whereas the Cp* ligands are omitted in the linear units.

Inorganic-Organometallic Hybrid Coordination Polymers

The unexpected coordination properties of **1** prompted us to investigate its coordination behavior towards CuI in the presence of P_4S_3. This cage molecule provides two P atoms of the basis and the apical P atom for the construction of a two-dimensional network in $(P_4S_3)(CuI)_3$.[18] In a control experiment the competitive reaction of [$Cp^*_2Mo_2P_4S$] and P_4S_3 with CuI has been investigated.

[$(Cp°_2Mo_2P_4S)(P_4S_3)(CuI)_2]_n$

The reaction of a mixture of **1**, P_4S_3 and CH_2Cl_2 with a solution of CuI in MeCN gave two different kinds of red platelets which were separated manually. X-ray diffraction structure analysis revealed that compounds **7** and **8** have similar composition [$(Cp°_2Mo_2P_4S)(P_4S_3)(CuI)_2]_n$. Accordingly, elemental analysis of the crystalline material reflects the composition of the mixture.

The crystal structures of both compounds **7** and **8** contain linear strands of [$\mathbf{1}(CuI)_2]_n$ and [$(P_4S_3)(CuI)_2]_n$, which are linked by planar Cu$_2$I$_2$ four-membered rings (see Figures 6, 8). Both the inorganic and organometallic building blocks are *trans*-connected by this ring giving rise to a crosswise pattern of strands within the *ac* plane. It is striking that in the structure of **7** the apical P atoms (P5) of the cage molecules point in the same direction. The coordination of the *cyclo*-P$_4$S middle deck is achieved by P1 of the η^3-P$_3$ and P4 of the η^2-PS ligands and the Cp° ligands are oriented approximately parallel with respect to the *ac* plane in **7** (Figure 7).

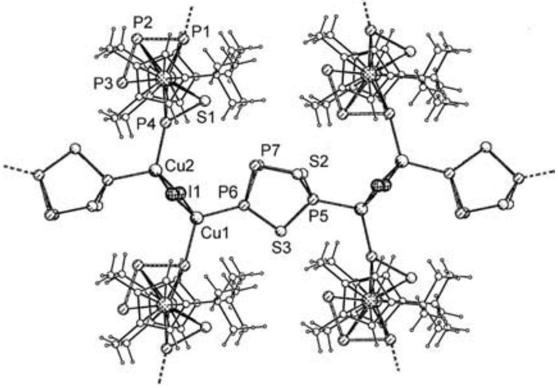

Figure 6. Section of the crystal structure of 2D-[(Cp°$_2$Mo$_2$P$_4$S)(P$_4$S$_3$)(CuI)$_2$]$_n$ (**7**). Selected distances [Å] in **7**: Mo–Mo 2.673(1), Mo–P 2.396(2)–2.621(2), Mo–S$_{\text{mean}}$ 2.483(2), S1–P4 2.071(4), S–P (P$_4$S$_3$)$_{\text{mean}}$ 2.095(3), P1–P2 2.172(4), P2–P3 2.132(3), P6–P7 2.219(3), P7–P7a 2.241(4), Cu–I$_{\text{mean}}$ 2.645(1), Cu–P$_{\text{mean}}$ 2.271(3), Cu1···Cu2 2.907(1).

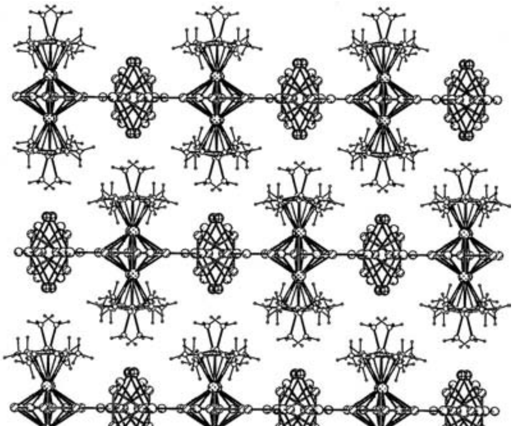

Figure 7. Section of the crystal structure of **7**; view down the *a*-axis.

The structure of **8** differs from that of **7** by an alternate orientation of the P$_4$S$_3$ cages (Figure 8). Other differences are incorporation of CH$_2$Cl$_2$ molecules between the layers and the tilted Mo–Mo axes by 11° with respect to the *bc* plane what also affects the packing of the Cp° ligands. Concomitantly, there is a simultaneous disorder of P$_4$S$_3$ cages and Cu$_2$I$_2$ rings caused by a switch of the coordination sites from one P atom (P5) to the other (P6) within the P$_3$ basis. The most striking difference between the structures of **7** and **8** is that P$_4$S$_3$ undergoes a reorientational switch from one Cu$_2$I$_2$ ring to the other. As a consequence the coordination sites of the basis P atoms are involved as well as the inclination angles of the four-membered rings and the main-group atoms of the *cyclo*-P$_4$S middle decks within each strand.

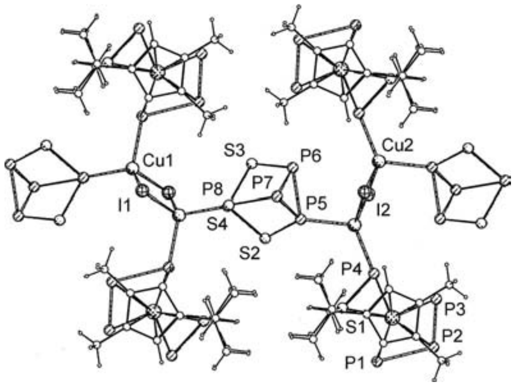

Figure 8. Section of the triclinic structure of **8**; P2 is covered by S4. Only the 67% majority of the polymer (see text) is shown; solvent molecules are omitted for clarity. Selected distances [Å]: Mo–Mo 2.683(1), S–P 1.972(6)–2.21(2), P–P 2.051(6)–2.503(7), Cu–P 2.236(2)–2.312(5), Cu–I 2.607(1)–2.659(1), Cu···Cu$_{\text{mean}}$ 2.878(1).

[(Cp*$_2$Mo$_2$P$_4$S)(P$_4$S$_3$)(CuI)$_2$]$_n$

Red insoluble needles of composition [(Cp*$_2$Mo$_2$P$_4$S)(P$_4$S$_3$)(CuI)$_2$]$_n$ (**9**) were obtained by slow diffusion of a CH$_3$CN solution of CuI into a solution of equimolar amounts of [Cp*$_2$Mo$_2$P$_4$S] and P$_4$S$_3$ in CH$_2$Cl$_2$. The structure of **9** was determined by X-ray crystallography and the composition was confirmed by elemental analysis. The ^{31}P MAS NMR spectrum of **9** shows rather broad signals (Figure 9), but it is possible to identify the resonances of the different building blocks by comparison with spectra of [Cp*$_2$Mo$_2$P$_4$S][10] and P$_4$S$_3$-containing polymers, e.g. (P$_4$S$_3$)(CuI)$_3$.[7a] Thus, the signals at δ = –350, 300 and 330 ppm are part of the ABMX spectrum of [Cp*$_2$Mo$_2$P$_4$S], belonging to the η^3-P$_3$ ligand. Whereas two resonances are relatively sharp that at δ = 330 ppm is significantly broadened. Although the ^{31}P-$^{63/65}$Cu coupling of this signal cannot be resolved by simulation of the spectrum, it is clear from correlation with the crystallographic result that the lateral P atom P13 is coordinated to copper while P14 and P15 are not. Unfortunately, the signal of the η^2-PS dumbbell, which may be expected as a multiplet at δ = –110 ppm, is superposed by the very broad signal at δ = –100 ppm. The latter may be assigned to the P$_3$ basis of the P$_4$S$_3$ cage, which should give rise to a singlet and a multiplet. A coupling with copper may also be expected for the apical P atoms P4 and P8 what may explain the broad resonance centered at δ = 80 ppm. Corresponding chemical shifts for (P$_4$S$_3$)(CuI)$_3$ are 82.2 for the apical and –94.9 and –94.2 ppm for the basal P atoms, while the^{31}P-$^{63/65}$Cu coupling constants range from 700 to 1600 Hz.[7a]

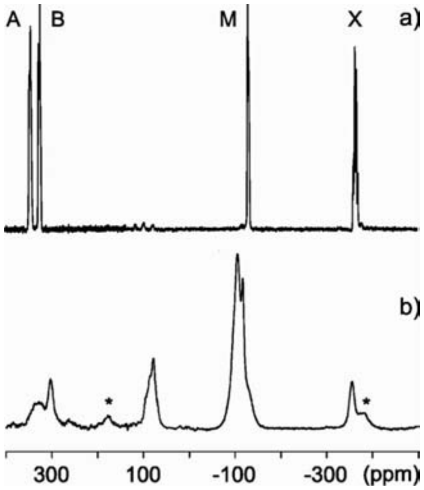

Figure 9. Comparison of experimental ^{31}P MAS NMR spectra of [Cp*$_2$Mo$_2$P$_4$S] (a; probe 2.5 mm, spinning frequency 30 kHz) and **9** (b; probe 2.5 mm, spinning frequency 34 kHz). Spinning side bands are indicated by an asterisk.

The crystal structure of **9** is composed of Cu$_2$I$_2$ four-membered rings bearing *trans*-coordinated P$_4$S$_3$ and tripledecker building blocks. Each P$_4$S$_3$ cage bridges two Cu$_2$I$_2$ rings by its apical P atom and one of the basal P atoms. The organometallic unit employs the lateral P atoms P13 (P9) of the η^3-P$_3$ ligand and adjacent P12 (P16) atoms of the η^2-PS dumbbell for coordination (Figure 10). This results in two sinoidal strands which are connected in an antiparallel manner to give 1D-ribbons. These are stacked in the crystal along the *a*-axis (Figure 11). Between these ribbons are two fairly huge solvent accessible voids of 968 Å^3, but it was not possible to build reasonable molecules from residual electron maxima. Compared to the structures of **7** and **8** P atoms in positions 3 and 4 contribute to coordination (Scheme 2) and not positions 1 and 4.

One crystallographic problem is inherent to many structures of molybdenum tripledecker complexes with a P$_4$S middle deck and P$_4$S$_3$ cages: both structural subunits tend to show positional disorder. In compound **9** here, where the middle deck is only fixed by two P atoms to the connecting copper, these P atoms statistically belong either to the PS dumbbell or to the P$_3$ fragment. This is in agreement with the originally found orthorhombic space group $Cmc2_1$ for **9**, in which only one symmetry independent P and Cu atom is possible to describe this binding situation. To elucidate this disorder situation, we decide to describe the structure in the monoclinic subgroup *C*1*c*1 wherein all five atoms of the middle deck can be described independently, inclusive their disorder. The refined occupation factor for the two orientation possibilities reaches a 53:47% statistic distribution.

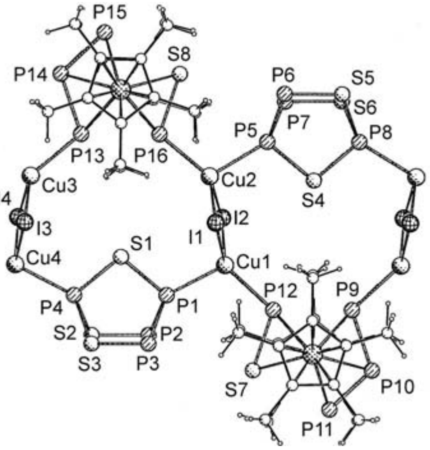

Figure 10. Section of the crystal structure of 1D-[(Cp*$_2$Mo$_2$P$_4$S)(P$_4$S$_3$)(CuI)$_2$]$_n$ (**9**). Only one set of the disordered main group elements is shown. Selected distances [Å]: Mo1–S7 2.507(6), Mo1–P9 2.434(7), Mo1–P10 2.522(6), Mo1–P11 2.449(11), Mo1–P12 2.429(7), Mo3–S8 2.516(8), Mo3–P13 2.419(6), Mo3–P14 2.516(8), Mo3–P15 2.415(14), Mo3–P16 2.425(6), S1–P1 2.090(10), S1–P4 2.068(9), S2–P2 1.962(14), S2–P4 2.120(8), S3–P3 1.990(12), S3–P4 2.137(10), S7–P12 2.185(9), P1–P3 2.139(10), P1–P2 2.122(8), P9–P10 2.179(9), P10–P11 2.085(15), Cu1–P1 2.320(9), Cu1–P12 2.260(8), Cu2–P5 2.276(9), Cu3–P13 2.272(7), Cu4–P4 2.309(8), I–Cu$_{\text{mean}}$ 2.62(1).

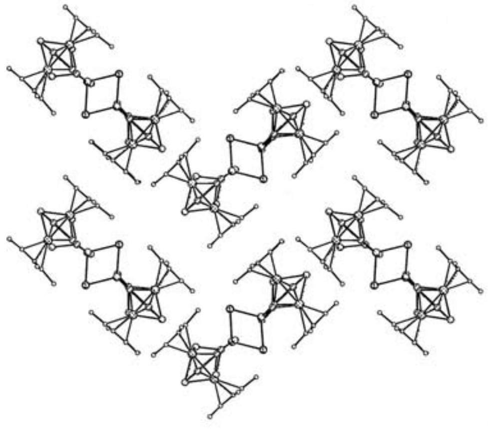

Figure 11. Section of the crystal structure of **9**; view down the *a*-axis.

The difficulty with the P$_4$S$_3$ cage is to distinguish between apical and basal P atoms, despite the fact, that normally the apical and one basal P atom are bound to copper. The situation in compound **9** is typical for this disorder, if it is described in space group *C*1*c*1: the two bound P atoms and the intermediate S atom are fully occupied and show normal displacement factors. For the remaining two S and two P atoms, eight-electron maxima are available. From distances to the already existent atoms and between the found maxima, one can clearly assign two sets of peaks to the missing basal P atoms or to the bridging S atoms. The refined occupation for the two orientations again nearly reaches statistic distribution with 54:46%.

Conclusions

In conclusion, the introduction of the Cp° ligand (Cp° = 1-*t*Bu-3,4-Me$_2$C$_5$H$_2$) into the chemistry of dimolybdenum tripledecker complexes with mixed group 15/16 element ligands gave among others [Cp°$_2$Mo$_2$P$_4$S] (**1**), which turned out as a new phosphorus-rich multifunctional building block in polymeric coordination chemistry.[19] A new type of dynamic helical porous metal-organic framework[20] has been formed by interaction of the *cyclo*-P_4S middle deck of **1** with CuI, which is able to reversibly absorb CH_2Cl_2 without loosing its crystalline character. The role of the secondary building unit[21] is taken over by the multi-functional organometallic complex **1** while bent Cu_2I_2 rings serve as inorganic knots. Attempts to introduce an inorganic linker into the system by adding P_4S_3 as competitive reagent gave one- and two-dimensional organometallic-inorganic hybrid polymers **7**–**9**. In these products planar Cu_2I_2 rings serve as knots combining inorganic and organometallic linkers in a surprisingly selective manner, what may open new perspectives for the synthesis of novel hybrid polymers.

Experimental Section

General: All manipulations were carried out under an inert atmosphere using Schlenk-line techniques and dry solvents. Elemental analyses were performed by the Mikroanalytisches Laboratorium, University of Regensburg. IR spectra were obtained with a Varian-Digilab Scimitar FTS800 spectrometer, FD mass spectra were measured on a Finnigan MAT95 spectrometer. The ^1H and ^{31}P NMR spectra were recorded on Bruker Avance 300 and 400 instruments, respectively. ^{31}P MAS NMR spectra were recorded on a Bruker Advance 300 spectrometer using a double resonance 2.5 mm MAS probe. The ^{31}P resonance was 121.495 MHz. The spectra were acquired at MAS rotation frequencies of 30 (**2**) and 34 kHz, a 90° pulse length of 2.3 µs and with relaxation delays between 120 and 450 s. $[Cp^{\circ}Mo(CO)_2]_2$ was prepared **via** decarbonylation of $[Cp^{\circ}Mo(CO)_3]_2$, whereas $[Cp^{\circ}Mo(CO)_3]_2$ was synthesized from $Mo(CO)_6$ and Cp°Li[22] in boiling THF, followed by subsequent oxidation of the resulting $Li[Cp^{\circ}Mo(CO)_3]$ according to standard procedures.[23]

Synthesis of $[Cp^{\circ}Mo(CO)_2]_2$: A mixture of Cp°Li (3.01 g, 19.27 mmol), $Mo(CO)_6$ (4.55 g, 17.23 mmol) and THF (100 mL) was refluxed for 19 h. After cooling of the dark red solution the solution of $Fe_2(SO_4)_3\cdot 9H_2O$ (10 g) and acetic acid (5 mL) in H_2O (100 mL) was added. Then the resulting bright-red precipitate of $[Cp^{\circ}Mo(CO)_3]_2$ (4.00 g, 6.07 mmol, 71%) was filtered, washed with water, acetone and Et_2O. The dry powder was suspended in toluene (150 mL) and then refluxed for 48 h. From time to time the flask was purged with N_2. After concentration the dark solution was filtered with toluene over SiO_2 (column 10 × 4 cm). After evaporation of the solvent red $[Cp^{\circ}Mo(CO)_2]_2$ [3.63 g, 6.03 mmol, 70% based on $Mo(CO)_6$] was obtained. ^1H NMR (300 MHz, C_6D_6): δ = 1.17 (s, 18 H, CMe_3), 1.83 (s, 12 H, Me), 4.68 (s, 4 H, CH) ppm. IR (KBr; ν_{CO}): $\tilde{\nu}$ = 1938 (vs), 1875 (vs), 1838 (vs) cm^{-1}. $C_{26}H_{34}Mo_2O_4$ (602.43): calcd. C 51.84, H 5.69; found C 51.54, H 5.72.

Reaction of $[Cp^{\circ}Mo(CO)_2]_2$ with P_4S_3: The suspension of $[Cp^{\circ}Mo(CO)_2]_2$ (1.15 g, 1.92 mmol) and P_4S_3 (0.42 g, 1.92 mmol) in toluene (100 mL) was refluxed for 17 h. After removal of the solvent the dark brown residue was chromatographed on SiO_2 (column 20 × 4 cm). With toluene two bands were eluted. Repeated chromatography of the first band (column 8 × 4 cm) gave after elution with pentane yellow $[Cp^{\circ}Mo(CO)_2P_3]$ (**3**; 65 mg, 4%), dark red $[Cp^{\circ}_2Mo_2P_4S]$ (**1**; 166 mg, 13%), and bright red $[Cp^{\circ}_2Mo_2(CO)_4P_2]$ (**4**; 98 mg, 8%). Low pressure chromatography of the second band (Merck Lobar Lichroprep Si60) gave after elution with toluene/pentane, 1:1 bright red $[Cp^{\circ}_2Mo_2P_2S_3]$ (**2**; 79 mg, 6%) and dark brown $[Cp^{\circ}_3Mo_3P_3S_4]$ (**5**; 39 mg, 3%). **1**: ^1H NMR (300 MHz, C_6D_6): δ = 1.19 (s, 18 H, CMe_3), 1.75 (s, 6 H, Me), 1.89 (s, 6 H, Me), 4.67 (s, 4 H, CH) ppm. $^{31}P\{^1H\}$ NMR (121 MHz, C_6D_6): δ = 344.1 (ddd; A), 323.3 (ddd; B), –150.9 (ddd; M); –386.6 (ddd, X); $J_{P,P}(AB)$ = 17, $J_{P,P}(AM)$ = 60, $J_{P,P}(AX)$ = 378, $J_{P,P}(BM)$ = 4, $J_{P,P}(BX)$ = 394, $J_{P,P}(MX)$ = 20 Hz ppm. FD MS (toluene): *m/z* = 646.1 [M^+]. $C_{22}H_{34}Mo_2P_4S$ (646.35): calcd. C 40.88, H 5.30, S 4.96; found C 41.20, H 5.34, S 4.83. **2**: ^1H NMR (300 MHz, C_6D_6): δ = 1.27 (s, 18 H, CMe_3), 1.99 (s, 12 H, Me), 5.37 (s, 4 H, CH) ppm. $^{31}P\{^1H\}$ NMR (121 MHz, C_6D_6): δ = –58.4 (s) ppm. ^{31}P MAS NMR (121 MHz): δ = –62.1 ppm. FD MS (toluene): *m/z* (%) = 324.0 (20) [M^{2+}], 647.1 (100) [M^+]. $C_{22}H_{34}Mo_2P_2S_3$ (648.54): calcd. C 40.74, H 5.28, S 14.83; found C 40.96, H 5.24, S 14.58. **3**: ^1H NMR (300 MHz, C_6D_6): δ = 0.98 (s, 9 H, CMe_3), 1.55 (s, 6 H, Me), 4.50 (s, 2 H, CH) ppm. $^{31}P\{^1H\}$ NMR (121 MHz, C_6D_6): δ = –333.8 (s) ppm. FD-MS (toluene): *m/z* = 396.1 [M^+]. IR (KBr; ν_{CO}): $\tilde{\nu}$ = 1986 (vs), 1947 (vs) **4**: ^1H NMR (300 MHz, C_6D_6): δ = 1.16 (s, 18 H, CMe_3), 1.82 (s, 12 H, Me), 4.68 (s, 4 H, CH) ppm. $^{31}P\{^1H\}$ NMR (121 MHz, C_6D_6): δ = –48.9 (s) ppm. FD MS (toluene): *m/z* = 664.2 [M^+]. IR (KBr; ν_{CO}): $\tilde{\nu}$ = 1980 (w), 1940 (sh), 1877 (s), 1837 (vs). **5**: ^1H NMR (300 MHz, C_6D_6): δ = 1.12 (s, 9 H, CMe_3), 1.17 (s, 9 H, CMe_3), 1.21 (s, 9 H, CMe_3), 1.86 (s, 6 H, Me), 2.04 (s, 6 H, Me), 2.17 (s, 6 H, Me), 4.90 (m, 2 H, CH), 4.91 (m, 1 H, CH), 4.92 (m, 1 H, CH), 5.26 (m, 1 H, CH), 5.27 (m, 1 H, CH) ppm. $^{31}P\{^1H\}$ NMR (121 MHz, C_6D_6): δ = 253.3 (t), –120.8 (d), $J_{P,P}$ = 19 Hz ppm. FD MS (toluene): *m/z* = 1012.3 [M^+]. IR (KBr; ν_{CO}): $\tilde{\nu}$ = 1918 (s), 1830 (s).

$[(Cp^{\circ}_2Mo_2P_4S)_3(CuI)_4]_n$ (6a): $Cp^{\circ}_2Mo_2P_4S$ (100 mg, 0.15 mmol) was dissolved in CH_2Cl_2 (10 mL) and layered with a solution of CuI (59 mg, 0.31 mmol) in CH_3CN. Dark rods of **6a** (yield 55 mg, 41%) were isolated, washed with diethyl ether and dried in vacuo. $C_{66}H_{102}Cu_4I_4Mo_6P_{12}S_3$ (2700.84): calcd. C 29.35, H 3.81, S 3.56; found C 29.22, H 3.49, S 3.55.

$[Cp^{\circ}_2Mo_2P_4S(P_4S_3)(CuI)_2]_n$ (7/8): A solution of **1** (75 mg, 0.12 mmol) and P_4S_3 (25 mg, 0.12 mmol) in CH_2Cl_2 (10 mL) was layered with a solution of CuI (44 mg, 0.24 mmol) in CH_3CN. Red-brown platelets consisting of a mixture of **7** and **8** (yield 40 mg, 27%) crystallized, which were separated manually. $C_{22}H_{34}Cu_2I_2Mo_2P_8S_4$ (1247.34): calcd. C 21.18, H 2.75, S 10.28; found C 20.85, H 2.34, S 10.33.

$[Cp^{*}_2Mo_2P_4S(P_4S_3)(CuI)_2]_n$ (9): A mixture of $[Cp^{*}_2Mo_2P_4S]$ (74 mg, 0.12 mmol), P_4S_3 (26 mg, 0.12 mmol) and CH_2Cl_2 (10 mL) was layered with a solution of CuI (45 mg, 0.24 mmol) in CH_3CN. Bright red needles of **9** (46 mg, 31%) were isolated, washed with diethyl ether and dried in vacuo. $C_{20}H_{30}Cu_2I_2Mo_2P_8S_4$ (1219.28): calcd. C 19.70, H 2.48, S 10.52; found C 19.56, H 2.52, S 10.26. ^{31}P MAS NMR (121 MHz): δ = –350 (m), –100 (m), 80 (m), 300 (s), 330 (m) ppm.

Crystal Structure Determination: Crystallographic data of the crystal structure determinations for **5**, **6**, **7**, **8**, and **9** are given in Table 1. The structures were solved by direct methods and refined on F^2 by full-matrix least-squares (SHELXL97 program) with all reflections. Hydrogen atoms were considered in calculated positions. Solvent molecules in the structures of **6a**, **8** and **9** are strongly disordered and could not be localized.

6a: The refined structure of **6a** contains eight large voids of 323 $Å^3$ and four small ones of 73 $Å^3$. Although the big void seems to be large enough for inclusion of solvent molecules, it looks "empty" because there are no big electron density peaks there and according to the PLATON/SQUEEZE calculations it contains only 10 e^-. **6b**:

Table 1. Crystallographic data of **5**–**9**.

	5	**6a**	**6b**
Formula	$C_{35}H_{51}Mo_3O_2P_3S_4$	$C_{66}H_{102}Cu_4I_4Mo_6P_{12}S_3$	$C_{66.55}H_{103.1}Cl_{1.1}Cu_4I_4Mo_6P_{12}S_3$
M_w	1012.8	2700.7	2747.4
Crystal size [mm^3]	$0.16 \times 0.05 \times 0.03$	$0.40 \times 0.35 \times 0.14$	$0.33 \times 0.28 \times 0.19$
Crystal system	monoclinic	tetragonal	tetragonal
Space group	$C2/c$	$I4_1/a$	$I4_1/a$
a [Å]	20.363(5)	31.316(1)	30.970(1)
b [Å]	24.524(5)	31.316(1)	30.970(1)
c [Å]	15.950(5)	19.907(1)	21.302(1)
α	–	–	–
β	93.6(1)	–	–
γ	–	–	–
V [Å^3]	7949(4)	19522.8(5)	20431.2(3)
Z	8	8	8
ρ_{cald} [g cm^{-3}]	1.692	1.839	1.786
μ [mm^{-1}]	10.981	19.665	19.056
λ [Å]	1.54184	1.54184	1.54184
Temperature [K]	123	123	123
Scan range	$2.82 < \Theta < 62.23$	$3.86 < \Theta < 66.56$	$3.81 < \Theta < 73.20$
Reflections collected	23431	18502	20612
Reflections observed [$I > 2\sigma(I)$]	5244	7260	7139
Parameters	439	452	484
Absorption correction	multi-scan	analytical	multi-scan
Transmission, min./max.	0.734/0.273	0.251/0.028	1/0.298
Residual density [e Å^{-3}]	0.083/–0.590	3.659/–1.700	2.680/–0.833
R_1, wR_2 ($I > 2\sigma$)	0.024/0.059	0.057/0.151	0.072/0.199
R_1, wR_2 (all data)	0.032/0.062	0.064/0.156	0.091/0.211

	7	**8**	**9**
Formula	$C_{11}H_{17}CuIMoP_4S_2$	$C_{24}H_{38}Cl_4Cu_2I_2Mo_2P_8S_4$	$C_{40}H_{60}Cu_4I_4Mo_4P_{16}S_8$
M_w	623.7	1417.1	2438.5
Crystal size [mm^3]	$0.17 \times 0.07 \times 0.02$	$0.25 \times 0.20 \times 0.03$	$0.36 \times 0.11 \times 0.02$
Crystal system	orthorhombic	triclinic	monoclinic
Space group	$Pnma$	$P\bar{1}$	Cc
a [Å]	19.124(1)	13.141(1)	13.346(1)
b [Å]	19.255(1)	13.512(1)	27.117(1)
c [Å]	10.409(1)	14.645(1)	23.186(1)
α	–	110.5(0)	–
β	–	97.3(1)	90
γ	–	107.5(1)	–
V [Å^3]	3833.0(3)	2242.5(1)	8391.1(3)
Z	8	2	4
ρ_{cald} [g cm^{-3}]	2.161	2.099	1.930
μ [mm^{-1}]	24.468	3.589	22.336
λ [Å]	1.54184	0.71073 (Mo-K_α)	1.54184
Temperature [K]	123	123	123
Scan range	$4.59 < \Theta < 67.14$	$3.08 < \Theta < 32.81$	$3.26 < \Theta < 66.60$
Reflections collected	8862	30887	11185
Reflections observed [$I > 2\sigma(I)$]	3132	10839	7383
Parameters	220	426	694
Absorption correction	analytical	analytical	multi-scan
Transmission, min./max.	0.624/0.153	0.701/0.421	1.000/0.030
Residual density [e Å^{-3}]	1.284/–0.719	3.026/–1.891	1.221/–1.025
R_1, wR_2 ($I > 2\sigma$)	0.030/0.078	0.043/0.103	0.055/0.144
R_1, wR_2 (all data)	0.033/0.081	0.064/0.107	0.065/0.151

The structure of the helical chains in **6b** is almost the same as in **6a** but the volume of both types of inter-chain voids increases from 323 to 477 Å^3 and from 73 to 90 Å^3, respectively. The residual electron density inside the big void increases significantly from 10 to 97 e$^-$ that roughly corresponds to two CH_2Cl_2 molecules. We approximated the electron density peaks in the big void of **6b** by two disordered CH_2Cl_2 molecules that partly occupy their positions. The resulting content of 0.55CH_2Cl_2 molecules per one formula unit is less than was predicted by PLATON probably because of serious positional disorder that cannot be fully approximated. **7**: The residual electron maxima give some hints that the P_4S middle deck shows the usual positional disorder, but to such a small amount that it can be ignored for this crystal. **8**: One of the two CH_2Cl_2 molecules in the structure of **8** could be refined, whereas the other one is located around the inversion center at (0, 0, 0.5) and must show disorder. **9**: Within the two solvent accessible voids in the unit cell of **9** SQUEEZE found 214 e$^-$ each, which may be filled with CH_3CN or CH_2Cl_2 or a mixture of both of them.

CCDC-791440 (for **6b**), -791441 (for **5**), -791442 (for **9**), -791443 (for **8**), -791444 (for **7**), -791445 (for **6a**) contain the supplementary crystallographic data for this paper. These data can be obtained free of charge from The Cambridge Crystallographic Data Centre via www.ccdc.cam.ac.uk/data_request/cif.

Acknowledgments

This work was supported by the Deutsche Forschungsgemeinschaft (DFG) (Wa 485/10-1). The authors also thank the European Union, COST action CM0802 (PhosSciNet) for financial support. Dr. Gabor Balázs is acknowledged for measurement and structure solution of **5**.

---

[1] R. Peng, M. Li, D. Li, *Coord. Chem. Rev.* **2010**, *254*, 1–18, and references cited therein.

[2] a) S. Hu, M.-L. Tong, *Dalton Trans.* **2005**, 1165–1167; b) E. Cariati, D. Roberto, R. Ugo, P. C. Ford, S. Galli, A. Sironi, *Inorg. Chem.* **2005**, *44*, 4077–4085; c) M. Bi, G. Li, Y. Zou, Z. Shi, S. Feng, *Inorg. Chem.* **2007**, *46*, 604–606; d) H. Araki, K. Tsuge, Y. Sasaki, S. Ishizaka, N. Kitamura, *Inorg. Chem.* **2007**, *46*, 10032–10034; e) J. He, J.-X. Zhang, C.-K. Tsang, Z. Xu, Y.-G. Yin, D. Li, *Inorg. Chem.* **2008**, *47*, 7948–7950.

[3] a) A. Vegas, J.-Y. Saillard, *Inorg. Chem.* **2004**, *43*, 4012–4018 and references cited therein; b) W.-F. Fu, X. Gan, C.-M. Che, Q.-Y. Cao, Z.-Y. Zhou, N. N.-Y. Zhu, *Chem. Eur. J.* **2004**, *10*, 2228–2236; c) M. Scherer, D. Stein, F. Breher, J. Geier, H. Schönberg, H. Grützmacher, *Z. Anorg. Allg. Chem.* **2005**, *631*, 2770–2774; d) R. D. Pike, P. D. Borne, J. T. Maeyer, A. L. Rheingold, *Inorg. Chem.* **2002**, *41*, 631–633; e) F. Cecconi, C. A. Ghilardi, S. Midollini, A. Orlandini, *J. Chem. Soc., Chem. Commun.* **1982**, 229–230; f) T. S. Lobana, P. Kaur, T. Nishioka, *Inorg. Chem.* **2004**, *43*, 3766–3767.

[4] a) P. C. Healy, B. W. Skelton, A. W. White, *J. Chem. Soc., Dalton Trans.* **1989**, 971–976; b) L. Chen, L. K. Thompson, S. S. Tandon, J. N. Bridson, *Inorg. Chem.* **1993**, *32*, 4063–4068; c) T. S. Lobana, G. Hundal, *J. Chem. Soc., Dalton Trans.* **2002**, 2203–2206; d) T. S. Lobana, Rimple, A. Castineiras, P. Turner, *Inorg. Chem.* **2003**, *42*, 4731–4737; e) J. Zhou, G.-Q. Bian, J. Dai, Y. Zhang, Q.-Y. Zhu, W. Lu, *Inorg. Chem.* **2006**, *45*, 8486–8488; f) S. Delgado, P. J. S. Miguel, J. L. Priego, R. Jimenez-Aparicio, C. J. Gómez-Garcia, F. Zamora, *Inorg. Chem.* **2008**, *47*, 9128–9130.

[5] a) H. Araki, K. Tsuge, Y. Sasaki, S. Ishizaka, N. Kitamura, *Inorg. Chem.* **2007**, *46*, 10032–10034; b) A. M. Kirillov, P. Smoleński, M. Haukka, M. F. C. Guedes da Silva, A. J. L. Pombeiro, *Organometallics* **2009**, *28*, 1683–1687; c) A. M. Kirillov, P. Smoleński, Z. Mha, M. F. C. Guedes da Silva, M. Haukka, A. J. L. Pombeiro, *Organometallics* **2009**, *28*, 6425–6431.

[6] a) J. J. M. Amoore, L. R. Hanton, M. D. Spicer, *Dalton Trans.* **2003**, 1056–1058; b) J. Wang, S.-L. Zheng, S. Hu, Y.-H. Zhang, M.-L. Tong, *Inorg. Chem.* **2007**, *46*, 795–800; c) S.-Q. Bai, L. L. Koh, T. S. A. Hor, *Inorg. Chem.* **2009**, *48*, 1207–1213.

[7] a) A. Biegerl, E. Brunner, C. Gröger, M. Scheer, J. Wachter, M. Zabel, *Chem. Eur. J.* **2007**, *13*, 9270–9276; b) A. Biegerl, C. Gröger, H. R. Kalbitzer, J. Wachter, M. Zabel, *Z. Anorg. Allg. Chem.* **2010**, *636*, 770–774; c) G. Balázs, A. Biegerl, C. Gröger, J. Wachter, R. Weihrich, M. Zabel, *Eur. J. Inorg. Chem.* **2010**, 1231–1237.

[8] a) A. Adolf, M. Gonsior, I. Krossing, *J. Am. Chem. Soc.* **2002**, *124*, 7111–7116; b) I. Raabe, S. Antonijevic, I. Krossing, *Chem. Eur. J.* **2007**, *13*, 7510–7522.

[9] H. Brunner, U. Klement, W. Meier, J. Wachter, O. Serhadle, M. L. Ziegler, *J. Organomet. Chem.* **1987**, *335*, 339–352.

[10] L. J. Gregoriades, G. Balázs, E. Brunner, C. Gröger, J. Wachter, M. Zabel, M. Scheer, *Angew. Chem.* **2007**, *119*, 6070; *Angew. Chem. Int. Ed.* **2007**, *46*, 5966–5970.

[11] C. Gröger, M. M. Kubicki, W. Meier, M. Pronold, J. Wachter, M. Zabel, *Organometallics* **2009**, *28*, 5633–5640.

[12] a) P. Sauvageot, C. Moïse, *Bull. Soc. Chim. Fr.* **1996**, *133*, 177–182; b) A. Sadorge, P. Sauvageot, O. Blacque, M. M. Kubicki, C. Moïse, L.-C. Leblanc, *J. Organomet. Chem.* **1999**, *575*, 278–285; c) G. Boni, O. Blacque, P. Sauvageot, N. Poujaud, C. Moïse, M. M. Kubicki, *Polyhedron* **2002**, *21*, 371–379.

[13] O. J. Scherer, H. Sitzmann, G. Wolmershauser, *Angew. Chem.* **1985**, *97*, 358; *Angew. Chem. Int. Ed. Engl.* **1985**, *24*, 351–352.

[14] a) O. J. Scherer, H. Sitzmann, G. Wolmershäuser, *J. Organomet. Chem.* **1984**, *268*, C9–C12; b) O. J. Scherer, H. Sitzmann, G. Wolmershäuser, *Acta Crystallogr., Sect. C* **1985**, *41*, 1761–1763; c) P. Jutzi, R. Kroos, *Chem. Ber.* **1988**, *121*, 1399–1401; d) M. Scheer, G. Friedrich, K. Schuster, *Angew. Chem.* **1993**, *105*, 641; *Angew. Chem. Int. Ed. Engl.* **1993**, *32*, 593–594; e) M. Scheer, K. Schuster, A. Krug, H. Hartung, *Chem. Ber./Recueil* **1997**, *130*, 1299–1304.

[15] a) O. Bumbu, C. Silvestru, M. C. Gimeno, A. Laguna, *J. Organomet. Chem.* **2004**, *689*, 1172–1179; b) M. Shafaei-Fallah, W. Shi, D. Fenske, A. Rothenberger, *Z. Anorg. Allg. Chem.* **2006**, *632*, 1091–1096; c) R. P. Davies, M. A. Gimenez, L. Patel, A. J. P. White, *Dalton Trans.* **2008**, 5705–5707.

[16] a) M. Munakata, T. Kuroda-Sowa, M. Maekawa, A. Hirota, S. Kitagawa, *Inorg. Chem.* **1995**, *34*, 2705–2710; b) P. V. Solntsev, J. Sieler, H. Krautscheid, K. V. Domasevitch, *Dalton Trans.* **2004**, 1153–1158; X.-Q. Wang, J.-K. Cheng, Y.-H. Wen, J. Zhang, Z.-J. Li, Y.-G. Yao, *Inorg. Chem. Commun.* **2005**, *8*, 897–899.

[17] P. Sluis, A. L. Spek, *Acta Crystallogr., Sect. A* **1990**, *46*, 194–201.

[18] J. Wachter, *Coord. Chem. Rev.* **2010**, *254*, 2078–2085.

[19] a) M. Scheer, *Dalton Trans.* **2008**, 4372–4386; b) J. Bai, A. V. Virovets, M. Scheer, *Angew. Chem.* **2002**, *114*, 1808; *Angew. Chem. Int. Ed.* **2002**, *41*, 1737–1740; c) J. Bai, A. V. Virovets, M. Scheer, *Science* **2003**, *300*, 781–783; d) M. Scheer, J. Bai, B.-P. Johnson, R. Merkle, A. V. Virovets, C. E. Anson, *Eur. J. Inorg. Chem.* **2005**, 4023–4026; e) M. Scheer, A. Schindler, J. Bai, B.-P. Johnson, R. Merkle, R. Winter, A. V. Virovets, E. V. Peresypkina, N. A. Blatov, M. Sierka, H. Eckert, *Chem. Eur. J.* **2010**, *16*, 2092–2107; f) M. Scheer, A. Schindler, C. Gröger, A. V. Virovets, E. V. Peresypkina, *Angew. Chem.* **2009**, *121*, 5148; *Angew. Chem. Int. Ed.* **2009**, *48*, 5046–5049; g) M. Scheer, A. Schindler, R. Merkle, B.-P. Johnson, M. Linseis, R. Winter, C. E. Anson, A. Virovets, *J. Am. Chem. Soc.* **2007**, *129*, 13386–13387; h) M. Scheer, L. J. Gregoriades, A. V. Virovets, W. Kunz, R. Neueder, I. Krossing, *Angew. Chem.* **2006**, *118*, 5818; *Angew. Chem. Int. Ed.* **2006**, *45*, 5689–5693.

[20] a) K. Biradha, A. Ramanan, J. J. Vittal, *Cryst. Growth Des.* **2009**, *9*, 2969–2970; b) C.-S. Lim, J. Jankolovits, J. W. Kempf, V. C. Pecoraro, *Chem. Asian J.* **2010**, *5*, 46–49.

[21] B. Chen, M. Eddaoudi, S. T. Hyde, M. O'Keeffe, O. M. Yaghi, *Science* **2001**, *291*, 1021–1023.

[22] J.-M. Conia, M.-L. Leriverend, *Bull. Soc. Chim. Fr.* **1970**, *3*, 2981–2991.

[23] A. R. Manning, P. Hackett, R. Birdwhistell, P. Soye, *Inorg. Synth.* **1990**, *28*, 148–150.

Received: October 21, 2010